


Cite this: *RSC Adv.*, 2020, 10, 18927

# Synthesis of some new acylhydrazone compounds containing the 1,2,4-triazole structure and their neuritogenic activities in Neuro-2a cells†

Xia Jiang,<sup>ab</sup> Genyun Tang,<sup>c</sup> Jie Yang,<sup>b</sup> Jiacheng Ding,<sup>b</sup> Hongwei Lin<sup>\*b</sup> and Xiaoliang Xiang<sup>†a</sup>

In the present study, a novel series of acylhydrazone compounds (**A0–A10**) with the structure of 1,2,4-triazole have been designed and synthesized. In addition, all the synthesized compounds have been evaluated for neuritogenic activity in mouse neuroblastoma (Neuro-2a) cells. Notably, we found that one of these 11 acylhydrazone compounds, compound **A5** (2-(4-amino-5-(pyridin-4-yl)-4H-1,2,4-triazol-3-ylthio)-N'-(2-hydroxybenzylidene)-acetohydrazide) displays excellent neuritogenic activity. Moreover, our present study revealed that compound **A5** had the ability to induce neurite outgrowth through the PI3K/Akt and MEK-ERK signaling pathway in Neuro-2a cells. These findings suggest that compound **A5** might exert neuritogenic effects and thus may be useful for the treatment of neural repair and regeneration.

Received 1st April 2020  
Accepted 5th May 2020

DOI: 10.1039/d0ra02880k

rsc.li/rsc-advances

## 1. Introduction

The functions of the nervous system are mediated by neural circuits that are formed during brain development.<sup>1</sup> Neurite outgrowth is a critical cellular process underlying neural circuit formation.<sup>2</sup> It is well known that abnormalities of this process are associated with some neurodegenerative diseases. For instance, neurite atrophy is one of the typical symptoms in early stages of Alzheimer's and Parkinson's diseases.<sup>3–5</sup> Furthermore, neurite loss is one of the cardinal features of neuronal injury.<sup>6</sup> Therefore, it has been suggested that promoting neurite outgrowth is important when repairing nerve system damage, and it is necessary for the recovery of neuronal functions. So far, various compounds derived from bioactive natural products or chemical synthesis with potential neurite outgrowth have been studied for neuroregeneration.<sup>7,8</sup>

Acylhydrazone Schiff base was synthesized by the condensation of hydrazide with aldehyde or ketone, it has strong coordination ability, a wide spectrum of biological activities and

superior performance in various aspects, making it a promising therapeutic drug and functional material.<sup>9,10</sup> In recent years, researchers have found that acylhydrazone compounds exhibit many beneficial biological activities, such as anti-bacterial,<sup>11–13</sup> anti-inflammatory,<sup>14–16</sup> anti-viral<sup>17,18</sup> and anti-tumor activities.<sup>19–21</sup> However, there are currently few studies on the neuroactivity of acylhydrazone compounds.

In the present study, some new acylhydrazone compounds containing 1,2,4-triazole structure were synthesized, and their neurite outgrowth-promoting activities were investigated in the Neuro-2a cells. This cell line is commonly used as an *in vitro* model system to study neuronal differentiation, neurite outgrowth and neurotoxicological studies.

## 2. Results and discussion

### 2.1 Synthesis of acylhydrazone compounds

The compound **A0–A10** were designed and synthesized *via* the routes as shown in Scheme 1. Initially, isoniazide and potassium hydroxide were dissolved in ethanol, adding carbon disulfide to obtained potassium 2-isonicotinoylhydrazine-carbodithioate, which reacted with hydrazine hydrate under 143 °C to afford 4-amino-5-(pyridin-4-yl)-4H-1,2,4-triazole-3-thiol (**A0**). Secondly, ethyl 2-(4-amino-5-(pyridin-4-yl)-4H-pyrazol-3-ylthio) acetate (**A1**) was synthesized by reaction of compound **A0** and ethyl chloroacetate in sodium hydroxide solution. Thirdly, hydrazine hydrate and compound **A1** were refluxed in methanol to obtain 2-(4-amino-5-(pyridin-4-yl)-4H-pyrazol-3-ylthio) acetohydrazide (**A2**). Finally, compound **A2** was reacted with different structures of aldehydes to gain the target compounds **A3–A10**. Structural explanations of the final compounds were performed with IR, <sup>1</sup>H-NMR, <sup>13</sup>C-NMR and

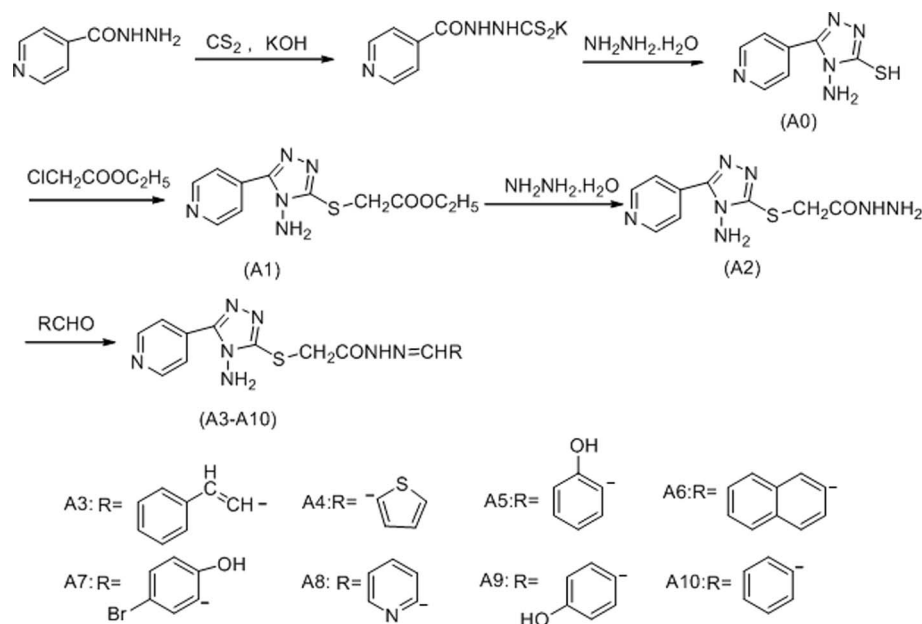
<sup>a</sup>Key Laboratory of Research and Utilization of Ethnomedicinal Plant Resources of Hunan Province, College of Biological and Food Engineering, Huaihua University, Huaihua 418008, P. R. China. E-mail: jiangxia285333006@163.com; xiangxiaoliang225@163.com

<sup>b</sup>Hunan Engineering Laboratory for Preparation Technology of Polyvinyl Alcohol (PVA) Fiber Material, College of Chemistry and Materials Engineering, Huaihua University, Huaihua 418008, P. R. China. E-mail: 1520224252@qq.com; 1471157054@qq.com; linhongwei1968@163.com

<sup>c</sup>School of Medicine, Hunan Provincial Key Laboratory of Dong Medicine, Hunan University of Medicine, Huaihua, Hunan 418000, P. R. China. E-mail: genyun1983311@126.com

† Electronic supplementary information (ESI) available. See DOI: 10.1039/d0ra02880k





Scheme 1 The synthetic routes to the target compounds (A0–A10).

GC-MS. In the IR spectra of the compounds, stretching absorptions around  $3300\text{ cm}^{-1}$  proved N–H bond of amino in the triazole and amide. Signals belonging to carbonyl ( $\text{C}=\text{O}$ ) function appeared at  $1651\text{--}1764\text{ cm}^{-1}$  (Amide I band), the absorption peak of another band of amide appeared near  $1265\text{ cm}^{-1}$ . The absorption at about  $1529\text{ to }1608\text{ cm}^{-1}$  was registered for  $\text{C}=\text{N}$  bonds. The out of plane bending belonging to substituted benzene was determined at  $794\text{--}833\text{ cm}^{-1}$ . In the  $^1\text{H}$ -NMR spectra, protons belonging to amide ( $\text{CONH}$ ) were observed as singlet peaks at 9.91 ppm and 11.99 ppm. Protons of methylene bridge ( $-\text{SCH}_2$ ) were recorded as singlet peaks between 4.10 ppm and 4.50 ppm. Amino groups on the triazole gave peaks between 6.30 ppm and 6.89 ppm. Protons of carbon–nitrogen double bond in hydrazone ( $-\text{CONHN}=\text{CH}-$ ) were recorded as singlet peaks between 7.57 ppm and 8.82 ppm. The target compounds **A3–A10** had *E/Z* geometric isomers and *cis-trans* conformation isomers, so in the absence of coupling, the proton signal peaks of  $\text{CONH}$ ,  $\text{SCH}_2$ ,  $\text{NH}_2$  and  $\text{N}=\text{CH}$  showed splitting. In  $^{13}\text{C}$ -NMR, carbons of methylene bridge ( $-\text{SCH}_2$ ) were recorded around 34.5 ppm. All aromatic carbons gave peaks from 110 ppm to 159 ppm. C3 of 1,2,4-triazole ring were recorded around 166 ppm and carbonyl group gave peaks over 168 ppm. In the GC-MS spectra, all masses were matched well with the expected  $\text{M} + \text{H}$  values.

## 2.2. Cytotoxic effects of acylhydrazone compounds on Neuro-2a cells

In addition to examination of the effects of acylhydrazone compounds on cell cytotoxicity, cell viability was determined by MTT assay (Fig. 1A). For this experiment, cells were seeded in wells of 96-well plate and maintained in culture medium for 24 h. The cells were then treated with test compounds (5, 10, 20, 50  $\mu\text{M}$  concentration of each compound) for 24 h. As indicated

in Fig. 1B, the compounds **A0**, **A1**, **A2**, **A3**, **A4**, **A5**, **A7** and **A8** showed that the dependence of cell viability on concentration is clearly noticed. Cytotoxic effects according to ISO 10993-5 standard,<sup>22</sup> if cell viability was above 80% are considered as non-cytotoxic; weak (60 to 80%); moderate (40 to 60%) and below 40% strong cytotoxicity, respectively. Among the tested compounds, **A0**, **A1**, **A2**, **A3**, **A4**, **A5** and **A8** showed no cytotoxic effect on Neuro-2a cells at 5  $\mu\text{M}$ , whereas, compounds **A7**, **A9** and **A10** showed weak cytotoxicity. Notably, compound **A6** exhibited strong cytotoxicity at this concentration. Therefore, a concentration of 5  $\mu\text{M}$  was used in subsequent experiments.

## 2.3 Effects of acylhydrazone compounds on neuronal differentiation of Neuro-2a cells

To investigate the influences of acylhydrazone compounds on neuronal differentiation. Neuro-2a cells were cultured in a low-serum (0.5% FBS) medium and treated with compounds **A0–A10** (5  $\mu\text{M}$ ) for 48 h. As shown in Fig. 2A, morphological changes were captured with phase contrast microscope. The differentiation rate and the longest length of neurite of each cell have been analyzed. As shown in Fig. 2B, only compound **A5** apparently induced Neuro-2a cells differentiation rate after 48 h treatment, whereas others were not. Fig. 2C shows that in addition to compound **A5**, compound **A7** also significantly promoted neurite outgrowth.

## 2.4 Effects of compound A5 on neuronal differentiation of Neuro-2a cells

As we revealed that compound **A5** had the neuritogenic activity, we then examined in detail the effect of compound **A5** on neurite outgrowth in Neuro-2a cells. The cells were treated with compound **A5** at the concentration of 1–10  $\mu\text{M}$  and cultured in differentiation medium for 48 h. As a positive control, retinoic



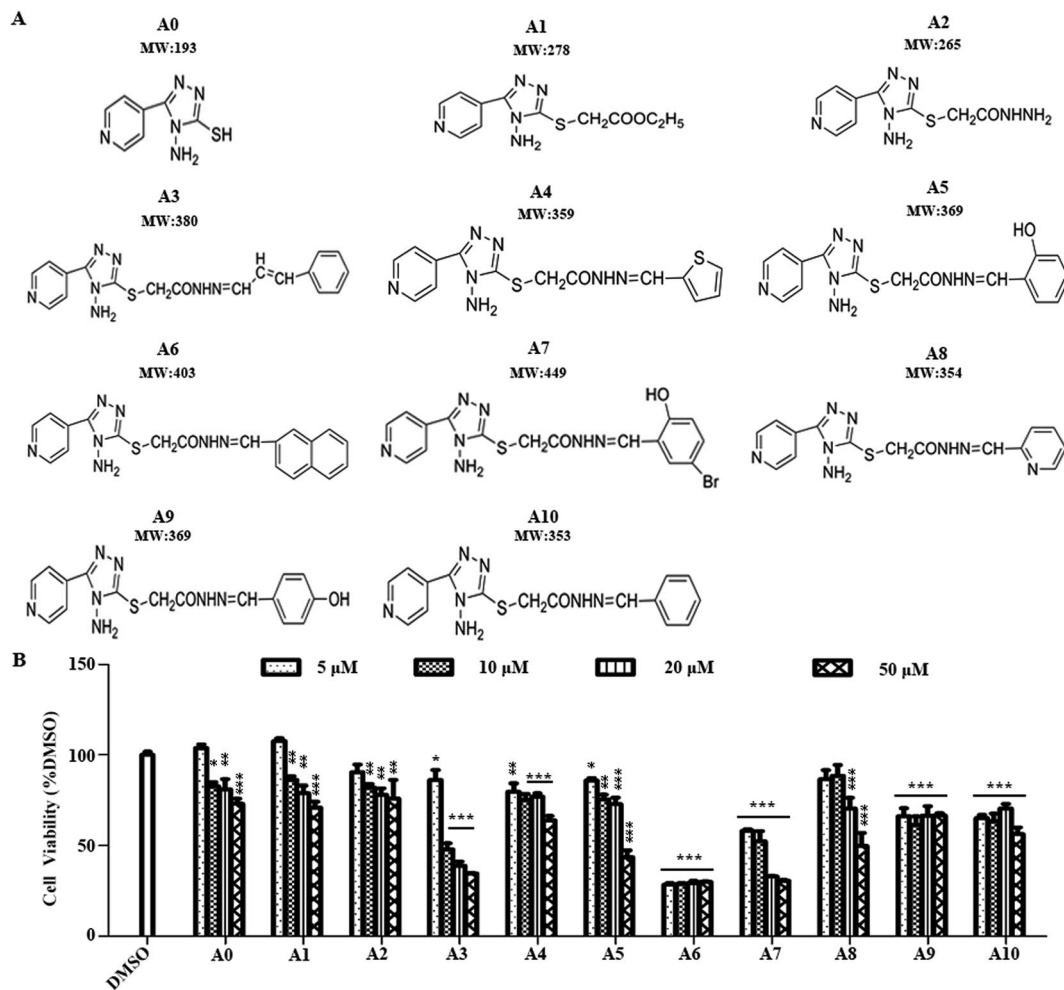


**Fig. 1** Cytotoxic effect of test compounds. (A) Chemical structures of compounds A0–A10. (B) Effect of test compounds on the viability of Neuro-2a cells. Neuro-2a cells treated with test compounds (compounds A0–A10 at different concentration (5–50 μM)). The results represent the mean ± SEM. ( $n = 5$ ). \* $P < 0.05$ , \*\* $P < 0.01$ , \*\*\* $P < 0.001$ , indicated compound vs. DMSO, one-way analysis of variance (ANOVA) followed by Tukey's test.

acid (RA) was used at the concentration of 10 μM. Fig. 3A shows the untreated cells (DMSO) having a round shape with few neurites and the RA-treated cells apparently displaying long neurites. Here, we compared the effect of the differentiation of Neuro-2a cells induced by A5 and RA. Notably, all aspects we examined, including differentiation rate (Fig. 3B) and the longest neurite length (Fig. 3C), A5 exhibited stronger activities as RA did. Moreover, compound A5 promoted neurite outgrowth in a concentration-dependent manner.

## 2.5 Signaling pathway involved in compound A5-induced neurite outgrowth from Neuro2a cells

To understand what signaling pathways functioning in the compound A5-induced neurite outgrowth, we treated Neuro-2a cells with A5 for different time points (0–240 min) and examined the levels of activated/phosphorylated forms of different signaling molecules (Fig. 4). Notably, compound A5 markedly activated extracellular signal regulated kinases 1/2 (ERK1/2) and p38 at 30 min treatment and thereafter. Examination of another

classical MAPK pathways revealed that c-Jun amino-terminal kinases (JNK) was not affected by compound A5. Besides up-regulating ERK1/2 and p38 pathways, the Akt pathway was slightly induced by A5.

To further determine the important signaling molecules that are required for compound A5 promoted neurite outgrowth, we took advantage of a series of pharmacological inhibitors, including LY294002 (PI3K inhibitor), U0126 (MEK1/2 inhibitor), BIRB795 (p38 inhibitor) and SP600125 (JNK inhibitor). We preincubated Neuro-2a cells with each of these inhibitors for 1 h before the treatment of compound A5, and the differentiation rate and the longest neurite length were examined (Fig. 5A). Consistent with the western blot analysis that ERK and Akt were activated by compound A5, the activities of ERK upstream kinases MEKs (MAPK/ERK kinase) and the Akt upstream kinase PI3K were both essentially required for compound A5 induced neurite outgrowth (Fig. 5B and C). By contrast, the activity of p38 was not important for compound A5's effect on promoting neurite outgrowth (Fig. 5B and C). Interestingly, although A5





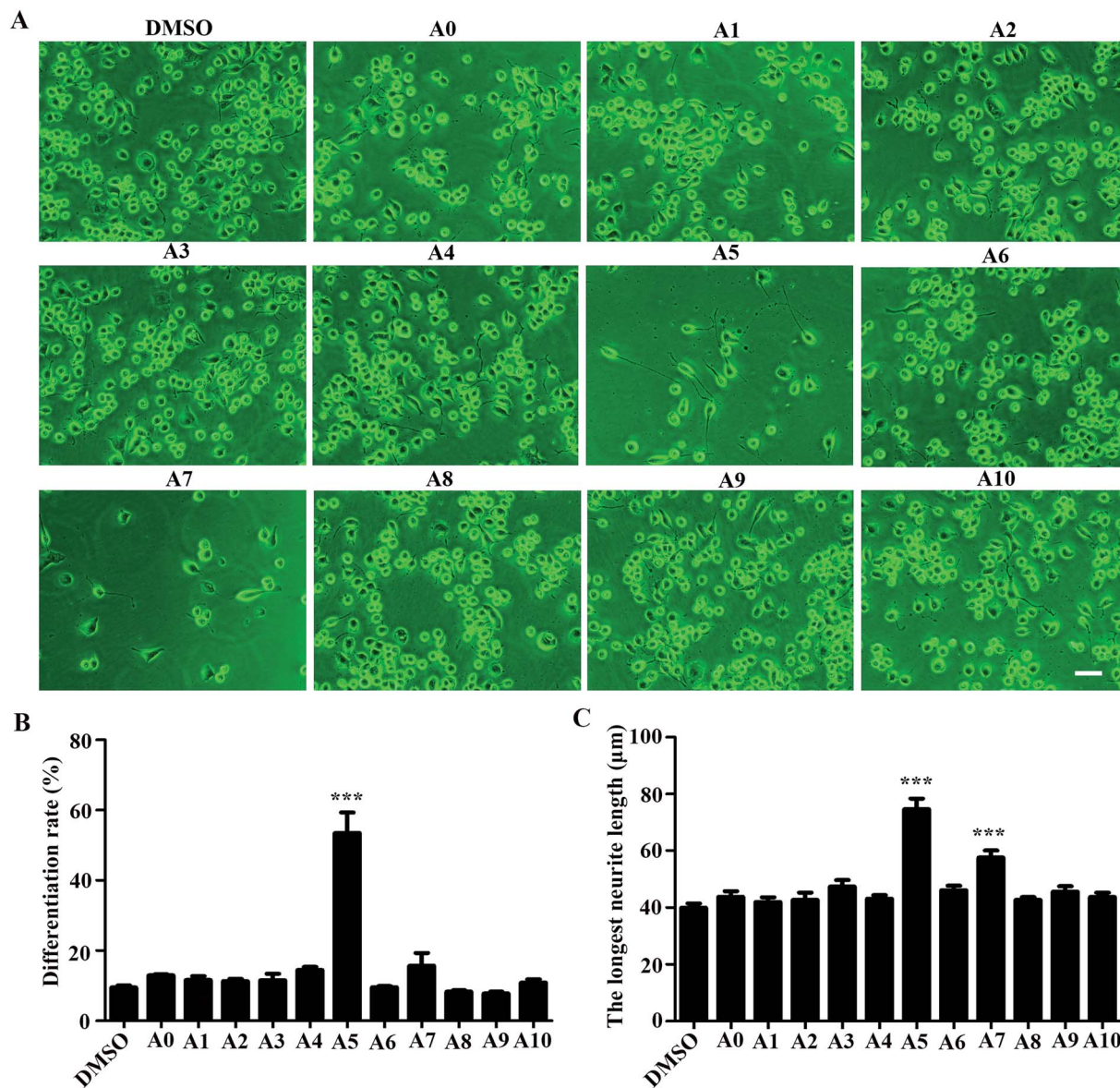


Fig. 2 Effect of Acylhydrazone compounds on the differentiation of Neuro-2a cells. (A) Neuro-2a cells were treated with different compounds (5 μM) for 48 h. Scale bar, 50 μm. The differentiation rate (B) and the longest neurite length of each differentiated cell (C) were analyzed. At least 400 cells/group were analyzed in each experiment ( $n = 3$ ), and values were presented as mean  $\pm$  SEM. \*\*\* $P < 0.001$ , indicated compound vs. DMSO, one-way analysis of variance (ANOVA) followed by Tukey's test.

does not affect the activity of JNK, but inhibition of JNK activity can offset the promotion of A5 on neurite growth (Fig. 5B and C). These results collectively suggest that compound A5 induces neuronal differentiation and neurite extension through activation of MEK-ERK and PI3K-Akt pathways, although the identity of the direct molecular target of A5 awaits further investigation.

### 3. Materials and methods

#### 3.1 Chemistry

All chemicals in this study were purchased from Shanghai Aladdin Reagent Company. A series of new acylhydrazone compounds containing 1,2,4-triazole (A0–A10) were synthesized

by the method previously reported.<sup>23,24</sup> The structures of the synthesised compounds were proved by  $^1\text{H-NMR}$ ,  $^{13}\text{C-NMR}$  and GC-MS. The  $^1\text{H-NMR}$  and  $^{13}\text{C-NMR}$  spectra were obtained in DMSO- $d_6$  by a Bruker Avance 400 MHz NMR spectrometer at 400 MHz and 100 MHz, respectively. The FT-IR spectra was recorded under ambient conditions in the wave number range of 4000–400  $\text{cm}^{-1}$  using an FT-IR Nicolet (Is5) spectrometer. GC-MS studies were performed on a GCMS-QP 2010 Plus (Shimadzu, Tokyo, Japan). Chemical purities of the compounds were checked by TLC applications performed on silica gel 60F<sub>254</sub>. The  $^1\text{H-NMR}$ ,  $^{13}\text{C-NMR}$  and GC-MS spectra of the compounds available in ESI†



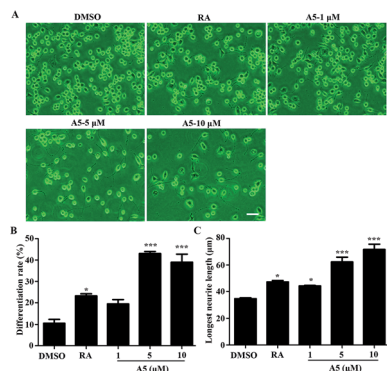


Fig. 3 Effect of compound A5 at different concentration on neurite outgrowth. Neuro-2a cells were treated with compound A5 at concentrations from 1 to 10  $\mu\text{M}$  for 48 h. (A) Representative images of Neuro-2a cells after treatment with compound A5. Scale bar, 50  $\mu\text{m}$ . The differentiation rate (B) and the longest neurite length of each differentiated cell (C) were analyzed. At least 400 cells/group were analyzed in each experiment ( $n = 3$ ), and values were presented as mean  $\pm$  SEM. \* $P < 0.05$ , \*\* $P < 0.01$ , \*\*\* $P < 0.001$ , indicated compound vs. DMSO, one-way ANOVA followed by Tukey's test.

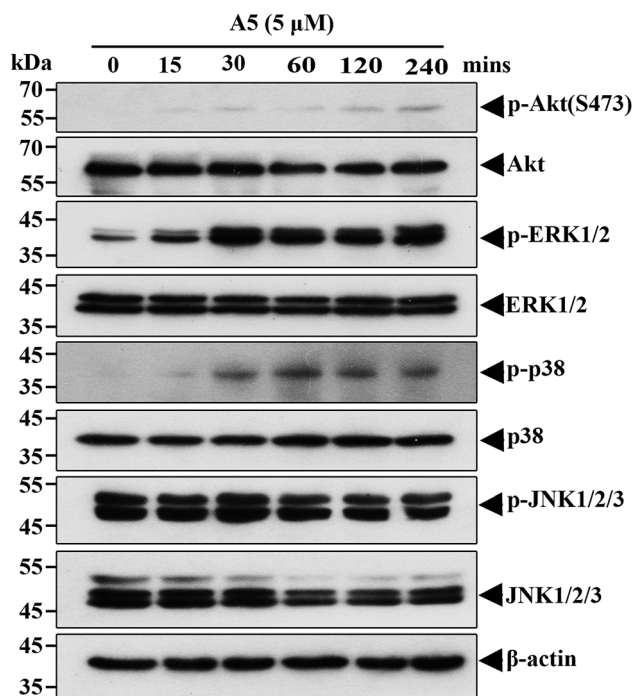


Fig. 4 Compound A5 increases phosphorylation levels of Akt, ERK1/2 and p38 in Neuro-2a cells. Compound A5 (5  $\mu\text{M}$ ) was added in Neuro-2a cells for indicated time points (0–240 min). Cells lysates were subjected to western blot analysis for the phosphorylated and total forms of different signaling molecules.

## 3.2 Synthesis

### 3.2.1 Synthesis procedure of 4-amino-5-(pyridin-4-yl)-4H-pyrazole-3-thiol (A0)

**Step 1: preparation of potassium 2-isonicotinoylhydrazinecarbodithioate.** KOH (7.80 g, 0.139 mmol) was added into absolute ethanol (150 mL) and stirred with heating until it

dissolved. The reaction mixture was cooled to room temperature. Then, isoniazid (10.04 g, 73.2 mmol) was added into the reaction mixture and 6 mL carbon disulfide ( $\text{CS}_2$ ) was slowly added dropwise. The mixture was stirred at room temperature for 10 h. The precipitated product was filtered and dried *in vacuo* to get the intermediate as a yellow powder.

**Step 2: preparation of 4-amino-5-(pyridin-4-yl)-4H-pyrazole-3-thiol (A0).** Potassium 2-isonicotinoylhydrazinecarbodithioate (12.99 g, 0.05 mol) was refluxed with 80% hydrazine hydrate (20 mL, 0.41 mol) in oil bath at 143  $^{\circ}\text{C}$  for 4 h. The obtained product was mixed with 20 mL distilled-ice water, and then adjust pH = 5 with concentrated hydrochloric acid. The obtained residue was filtered and dried *in vacuo* to get the compound A0 as white solid (yield, 77.6%).  $^1\text{H-NMR}$  (DMSO- $d_6$ , 400 MHz)  $\delta$ : 14.14 (s, 1H, -SH); 8.75–8.77 (d,  $J = 8$ , 2H, PyH); 8.02–8.03 (d,  $J = 4$ , 2H, PyH); 5.85 (s, 2H,  $\text{NH}_2$ ).  $^{13}\text{C-NMR}$  (DMSO- $d_6$ , 100 MHz): 168.08, 151.0, 150.59, 147.79, 133.40, 123.21, 121.05 MS (ESI)  $m/z$ : 193 ( $\text{M}^+$ ).

**3.2.2 Synthesis procedure of ethyl 2-(4-amino-5-(pyridin-4-yl)-4H-pyrazol-3-ylthio) acetate 9 (A1).** NaOH (1.93 g, 0.048 mol) was resolved in 45 mL distilled water. An amount of 4.89 g (0.025 mol) compound A0 was added. Then ethyl chloroacetate (5.60 mL, 0.045 mol) was slowly added dropwise. The mixture was stirred at 50  $^{\circ}\text{C}$  for 4 h. The mixture was cooled to room temperature, a precipitated product was crystallized, filtered and dried to give compound A1 as light-pink solid (yield, 40.9%).  $^1\text{H-NMR}$  (DMSO- $d_6$ , 400 MHz)  $\delta$ : 8.73–8.74 (d,  $J = 4$ , 2H, PyH); 7.98–7.99 (d,  $J = 4$ , 2H, PyH); 6.325 (s, 2H,  $\text{NH}_2$ ); 4.12–4.16 (m, 4H,  $\text{CH}_2$ ); 1.18–1.12 (m, 3H,  $\text{CH}_3$ ).  $^{13}\text{C-NMR}$  (DMSO- $d_6$ , 100 MHz): 168.45, 154.82, 152.57, 150.57, 134.32, 121.75, 61.73, 33.53, 14.46. MS (ESI)  $m/z$ : 279 ( $\text{M}^+$ ).

**3.2.3 Synthesis procedure of 2-(4-amino-5-(pyridin-4-yl)-4H-pyrazol-3-ylthio)acetohydrazide (A2).** Compound A1 (1.45 g, 5.2 mmol) was resolved in 35 mL anhydrous ethanol. An amount of 2.0 mL (0.41 mol) hydrazine hydrate (80%) was added. The solution was stirred and refluxed at 80  $^{\circ}\text{C}$  for 4 h. The mixture was cooled to room temperature, a precipitated product was crystallized, filtered and dried to give compound A2 as white solid (yield, 85.1%).  $^1\text{H-NMR}$  (DMSO- $d_6$ , 400 MHz)  $\delta$ : 9.34 (s, 1H, CONH); 8.73–8.74 (d,  $J = 4$ , 2H, PyH); 8.0–8.02 (d,  $J = 8$ , 2H, PyH); 6.30 (s, 2H, - $\text{NH}_2$ ); 4.32 (s, 2H, - $\text{NNH}_2$ ), 3.88 (s, 2H, - $\text{SCH}_2$ ).  $^{13}\text{C-NMR}$  (DMSO- $d_6$ , 100 MHz): 166.94, 154.93, 152.43, 150.57, 134.38, 121.79, 34.25. MS (ESI)  $m/z$ : 234.

**3.2.4 Synthesis procedure of acylhydrazone derivatives (A3–A10)**

**2-(4-Amino-5-(pyridin-4-yl)-4H-1,2,4-triazol-3-ylthio)-N'-(3-phenylallylidene) acetohydrazide (A3).** Compound A2 (0.21 g, 0.78 mmol) was resolved in 70 mL anhydrous ethanol. Then, cinnamaldehyde (0.18 mL, 1.43 mmol) was slowly added dropwise. The solution was stirred and refluxed at 67  $^{\circ}\text{C}$  for 4 h. The reaction mixture obtained was a clear and transparent solution. The mixture was cooled to room temperature and a solid separates out. Separated solid was filtered, dried and recrystallized by absolute ethanol to give compound A3 as white crystal (yield, 38.1%).  $^1\text{H-NMR}$  (DMSO- $d_6$ , 400 MHz)  $\delta$ : 11.65 (cis), 11.56 (trans) (s, 1H, CONH); 8.70–8.74 (m, 2H, PyH); 7.99–8.01 (d,  $J = 8$ , 2H, PyH); 7.57–7.59 (d,  $J = 8$ , 1H,  $\text{N}=\text{CH}$ ); 7.37–





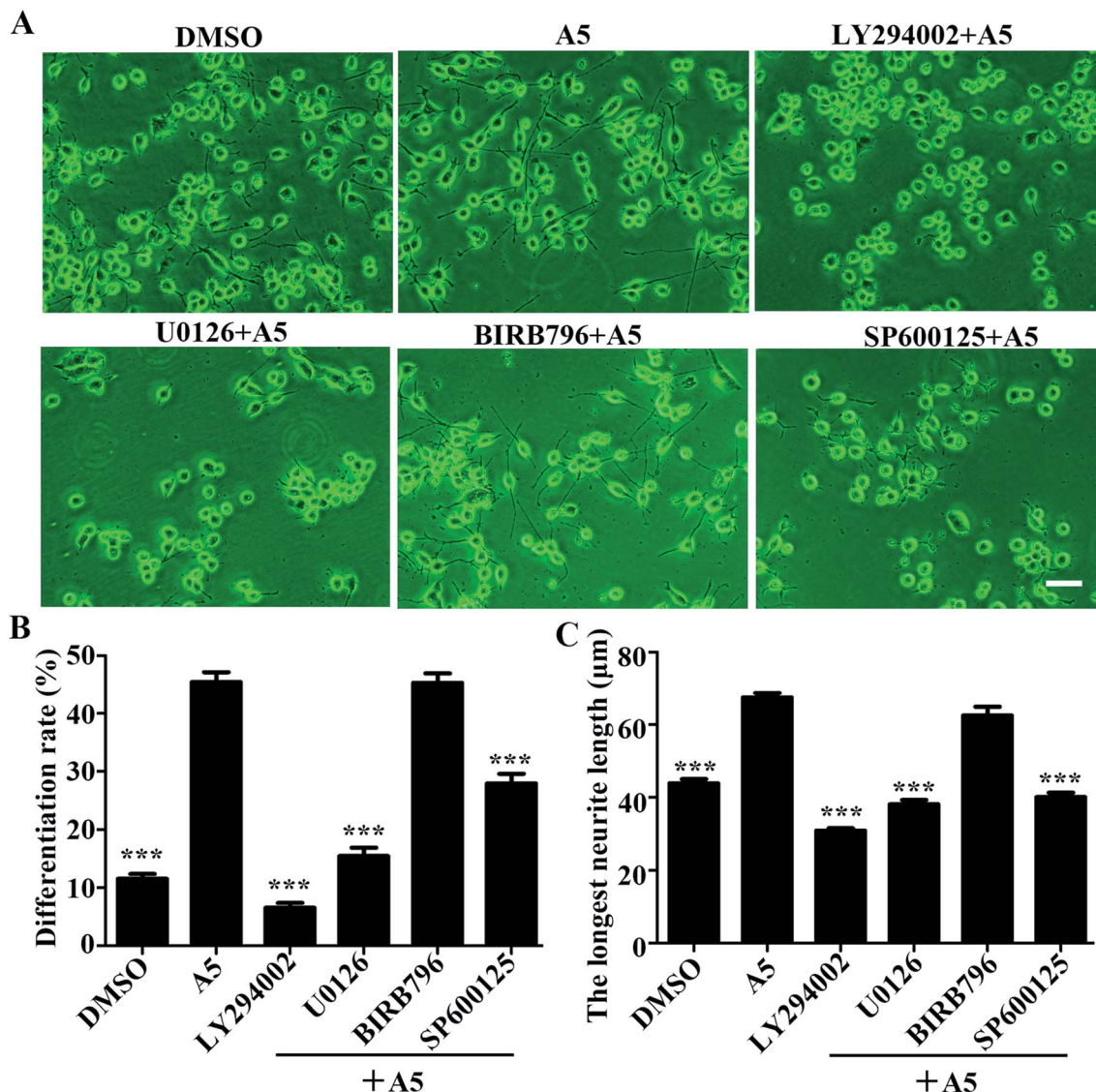


Fig. 5 Activation of MEK-ERK, PI3K-Akt and JNK1/2/3 signaling pathway is required for compound A5 induced neurite outgrowth. Neuro-2a cells were pretreated with different inhibitors, including PI3K inhibitor (LY290042, 10 μM), MEK inhibitor (U0126, 10 μM), p38 inhibitor (BIRB796, 10 μM) or JNK inhibitor (SP600125, 10 μM) for 1 h, followed by compound A5 treatment (5 μM) for 48 h. (A) Neurites were visualized by inverted phase contrast microscope. Cell differentiation rate (B) and the longest length of neurites per differentiated cell (C) were quantified. At least 400 cells/group were analyzed in each experiment ( $n = 3$ ), and values were presented as mean  $\pm$  SEM. \*\*\* $P < 0.001$ , DMSO or inhibitor and compound A5 cotreatment vs. compound A5 single treatment.

7.39 (d,  $J = 8$ , 2H,  $-\text{CH}=\text{CH}$ ); 7.35 (m, 3H, Ph-H); 7.33 (m, 2H, Ph-H); 6.32 (s, 2H,  $-\text{NH}_2$ ); 4.01 (*cis*), 4.41 (*trans*) (s, 2H,  $-\text{SCH}_2$ ). *trans/cis*: 5/4;  $^{13}\text{C}$ -NMR (DMSO- $d_6$ , 100 MHz)  $\delta$ : 169.05, 164.03, 155.10, 155.02, 152.52, 152.41, 150.58, 150.55, 149.51, 146.87, 139.84, 139.55, 136.27, 134.39, 129.31, 129.26, 127.57, 127.53, 125.77, 125.45, 121.77, 4.69 (*trans*), 34.63 (*cis*). MS (ESI)  $m/z$ : 380.0 ( $\text{M}^+$ ) IR (KBr)  $\nu$ : 3332, 3201, 1764, 1529.3.

The syntheses of compounds A4–A10 were carried out by the same procedure as described for the preparation of A3.

2-(4-Amino-5-(pyridin-4-yl)-4H-1,2,4-triazol-3-ylthio)- $N'$ -(thiophen-2-ylmethylene)acetohydrazide (A4). White crystal (yield, 28.41%).  $^1\text{H}$ -NMR (DMSO- $d_6$ , 400 MHz)  $\delta$ : 11.64 (*trans*), 11.72 (*cis*) (s, 1H, CONH); 8.73 (s, 2H, PyH); 8.42 (*trans*), 8.21 (*cis*) (s, 1H,  $\text{N}=\text{CH}$ );

7.99 (s, 2H, PyH); 7.64–7.66 (m, 1H, thiophen-H); 7.45–7.48 (m, 1H, thiophen-H); 7.11–7.12 (s, 1H, thiophen-H); 6.31–6.33 (d,  $J = 8$ , 2H,  $-\text{NH}_2$ ) 4.07 (*cis*), 4.22 (*trans*) (s, 2H,  $-\text{SCH}_2$ ); *trans/cis*: 10/11;  $^{13}\text{C}$ -NMR (DMSO- $d_6$ , 100 MHz)  $\delta$ : 168.96, 164.02, 155.15, 155.05, 152.51, 152.41, 150.57, 150.54, 142.73, 139.42, 139.21, 139.07, 134.41, 134.34, 131.65, 131.07, 129.53, 129.07, 128.39, 128.33, 121.78, 34.70 (*trans*), 34.30 (*cis*). MS (ESI)  $m/z$ : 359.0 ( $\text{M}^+$ ) IR (KBr)  $\nu$ : 3329, 3039, 2930, 1651, 1543, 1265.

2-(4-Amino-5-(pyridin-4-yl)-4H-1,2,4-triazol-3-ylthio)- $N'$ -(2-hydroxybenzylidene)acetohydrazide (A5). White flake solid (yield, 78.5%).  $^1\text{H}$ -NMR (DMSO- $d_6$ , 400 MHz)  $\delta$ : 12.05 (*cis*), 11.67 (*trans*) (s, 1H,  $-\text{ph}-\text{OH}$ ); 11.02 (*trans*), 10.11 (*cis*) (s, 1H, CONH); 8.77 (s, 2H, PyH), 8.03 (s, 2H, PyH); 8.46 (*cis*), 8.37



(*trans*) (s, 1H, N=CH); 7.26–7.33 (m, 2H, Ph-H), 7.59–7.60 (d, *J* = 4, 1H, Ph-H), 7.72–7.74 (d, *J* = 8, 1H, Ph-H); 6.37–6.39 (d, *J* = 8, *trans*), 6.89–6.96 (m, *cis*) (2H, -NH<sub>2</sub>); 4.52 (*trans*), 4.14 (*cis*) (s, 2H, -SCH<sub>2</sub>). *trans/cis*: 15/16. <sup>13</sup>C-NMR (DMSO-d<sub>6</sub>, 100 MHz)  $\delta$ : 169.03, 164.08, 157.74, 156.88, 155.19, 155.14, 152.57, 152.44, 150.61, 150.58, 147.57, 141.69, 134.41, 134.33, 131.98, 131.73, 129.61, 126.71, 121.79, 120.50, 119.90, 119.85, 119.11, 116.82, 116.61, 34.52 (*trans*), 34.33 (*cis*). MS (ESI) *m/z*: 369.0 (M<sup>+</sup>) IR (KBr)  $\nu$ : 3425, 3309, 3202, 2930, 1666, 1582, 1265.

**2-(4-Amino-5-(pyridin-4-yl)-4H-1,2,4-triazol-3-ylthio)-N'-(naphthalen-1-ylmethylene)acetohydrazide (A6).** White crystal (yield, 79.2%). <sup>1</sup>H-NMR (DMSO-d<sub>6</sub>, 400 MHz)  $\delta$ : 11.87 (*cis*), 11.72 (*trans*) (s, 1H, CONH); 8.72–8.82 (m, 4H, PyH); 8.59–8.62 (d, *J* = 12, 1H, N=CH); 7.96–7.98 (m, 4H, naphthalene-H); 7.60–7.64 (m, 3H, naphthalene-H); 6.33–6.35 (d, *J* = 8, 2H, -NH<sub>2</sub>); 4.15 (*cis*), 4.58 (*trans*) (s, 2H, -SCH<sub>2</sub>). *trans/cis*: 5/4; <sup>13</sup>C-NMR (DMSO-d<sub>6</sub>, 100 MHz)  $\delta$ : 169.37, 164.32, 155.13, 152.47, 150.52, 147.69, 143.90, 134.39, 133.95, 131.16, 130.89, 130.60, 129.75, 129.70, 129.30, 129.25, 128.70, 127.81, 127.47, 126.71, 125.96, 124.96, 124.07, 121.82, 121.75, 34.89 (*trans*), 34.63 (*cis*). MS (ESI) *m/z*: 403.0 (M<sup>+</sup>) IR (KBr)  $\nu$ : 3320, 3089, 2930, 1685, 1593, 1357.

**2-(4-Amino-5-(pyridin-4-yl)-4H-pyrazol-3-ylthio)-N'-(5-bromo-2-hydroxybenzylidene)acetohydrazide (A7).** White powder (yield, 32.38%). <sup>1</sup>H-NMR (DMSO-d<sub>6</sub>, 400 MHz)  $\delta$ : 12.06 (*cis*), 11.66 (*trans*) (s, 1H, -ph-OH); 11.04 (*cis*), 10.37 (*trans*) (s, 1H, CONH); 8.73 (s, 2H, PyH); 8.39 (*cis*), 8.25 (*trans*) (s, 1H, N=CH); 8.0 (s, 2H, PyH); 7.43–7.82 (m, 3H, Ph-H); 6.85 (*cis*), 6.32 (*trans*) (s, 2H, -NH<sub>2</sub>); 4.10 (*cis*), 4.49 (*trans*) (s, 2H, -SCH<sub>2</sub>). *trans/cis*: 20/19; <sup>13</sup>C-NMR (DMSO-d<sub>6</sub>, 100 MHz)  $\delta$ : 169.24, 164.28, 155.03, 152.55, 152.39, 150.57, 150.51, 145.21, 139.72, 134.40, 134.12, 133.90, 133.70, 130.70, 128.24, 122.95, 121.77, 121.66, 119.10, 118.87, 111.32, 110.94, 34.45 (*trans*), 34.41 (*cis*). MS (ESI) *m/z*: 449.0 (M<sup>+</sup>) IR (KBr)  $\nu$ : 3340, 3279, 2970, 1681, 1550, 1357.

**2-(4-Amino-5-(pyridin-4-yl)-4H-pyrazol-3-ylthio)-N'-(pyridin-2-ylmethylene)acetohydrazide (A8).** White powder (yield, 85.1%). <sup>1</sup>H-NMR (DMSO-d<sub>6</sub>, 400 MHz)  $\delta$ : 11.99 (*cis*), 11.85 (*trans*) (s, 1H, CONH); 8.71–8.74 (m, 2H, PyH); 8.58–8.61 (m, 1H, PyH); 8.22 (*cis*), 8.05 (*trans*) (s, 1H, N=CH); 7.81–7.97 (m, 4H, PyH); 7.37–7.44 (m, 1H, PyH); 6.34 (s, 2H, -NH<sub>2</sub>); 4.12 (*cis*), 4.51 (*trans*) (s, 2H, -SCH<sub>2</sub>); *trans/cis*: 8/5; <sup>13</sup>C-NMR (DMSO-d<sub>6</sub>, 100 MHz)  $\delta$ : 172.48, 169.64, 164.54, 155.06, 154.85, 153.39, 153.19, 152.54, 152.43, 150.48, 149.94, 147.78, 144.64, 137.37, 137.29, 134.40, 124.97, 124.79, 121.75, 120.46, 120.30, 34.67 (*trans*), 34.24 (*cis*). MS (ESI) *m/z*: 354.0 (M<sup>+</sup>) IR (KBr)  $\nu$ : 3340, 3197, 2930, 1689, 1608, 1377.

**2-(4-Amino-5-(pyridin-4-yl)-4H-pyrazol-3-ylthio)-N'-(4-hydroxybenzylidene)acetohydrazide (A9).** White powder (yield, 60.2%). <sup>1</sup>H-NMR (DMSO-d<sub>6</sub>, 400 MHz)  $\delta$ : 11.55 (*cis*), 11.46 (*trans*) (s, 1H, -ph-OH); 9.91 (*cis*), 9.88 (*trans*) (s, 1H, CONH); 8.73 (s, 2H, PyH), 7.98–8.0 (d, *J* = 8, 2H, PyH); 8.09 (*cis*), 7.92 (*trans*) (s, 1H, N=CH); 7.50–7.53 (d, *J* = 12, 2H, Ph-H); 6.80–6.82 (d, *J* = 8, 2H, Ph-H); 6.31–6.32 (s, 2H, -NH<sub>2</sub>); 4.06 (*cis*), 4.46 (*trans*) (s, 2H, -SCH<sub>2</sub>); *trans/cis*: 10/6; <sup>13</sup>C-NMR (DMSO-d<sub>6</sub>, 100 MHz)  $\delta$ : 168.99, 163.81, 159.96, 159.78, 155.09, 152.40, 150.53, 147.92, 144.62, 134.42, 129.38, 129.08, 125.43, 121.77, 116.16, 34.82 (*trans*), 34.62 (*cis*). MS (ESI) *m/z*: 369.0 (M<sup>+</sup>) IR (KBr)  $\nu$ : 3437, 3321, 3190, 1651, 1582, 1265.

**2-(4-Amino-5-(pyridin-4-yl)-4H-pyrazol-3-ylthio)-N'-benzylideneacetohydrazide (A10).** White powder (yield, 20.13%). <sup>1</sup>H-NMR (DMSO-d<sub>6</sub>, 400 MHz)  $\delta$ : 11.77 (*cis*), 11.66 (*trans*) (s, 1H, CONH); 8.73 (s, 2H, PyH); 8.21 (s, 1H, N=CH); 7.99–8.03 (d, *J* = 16, 2H, PyH); 7.69 (s, 2H, Ph-H); 7.42 (s, 3H, Ph-H); 6.32 (s, 2H, -NH<sub>2</sub>); 4.09 (*cis*), 4.50 (*trans*) (s, 2H, -SCH<sub>2</sub>); *trans/cis*: 8/5; <sup>13</sup>C-NMR (DMSO-d<sub>6</sub>, 100 MHz)  $\delta$ : 169.38, 164.20, 155.08, 152.51, 152.41, 150.53, 147.56, 144.27, 134.41, 130.62, 130.43, 129.27, 127.59, 127.34, 121.75, 34.74 (*trans*), 34.46 (*cis*). MS (ESI) *m/z*: 352.0 (M<sup>+</sup>) IR (KBr)  $\nu$ : 3250, 3035, 1662, 1552, 1307.

### 3.3 Cell culture

Mouse neuroblastoma Neuro-2a cell line was obtained from ATCC (Manassas, VA, United States) and cultured in MEM medium supplemented with 1% penicillin/streptomycin and 10% heat-inactivated fetal bovine serum at 37 °C in a humidified 5% CO<sub>2</sub> atmosphere. Cells were passaged every 3–4 days.

### 3.4 Cell viability assay

Cell viability was determined by MTT reduction assay. For assay,  $5 \times 10^3$  cells were plated in 96-well microtiter plates and grown for 24 h. Afterwards cells were treated with different concentrations of test compounds (5, 10, 20 and 50  $\mu$ M). After 24 h incubation, 10  $\mu$ L of stock MTT (5 mg mL<sup>-1</sup>) was added to each well and further incubated for four hours, and then the medium in the wells was removed and 200  $\mu$ L DMSO was added to each well. The absorbance was measured by a microplate reader at 570 nm. Cell viability was shown relative to the control in a graph.

### 3.5 Neurite outgrowth-promoting assay

For neurite outgrowth assay, Neuro-2a cells were seeded into 24-well plates at a density of  $1 \times 10^4$  cells per mL and grown for 24 h. After 24 h incubation, the culture medium was replaced with differentiation medium (MEM supplied with 0.5% FBS and 1% penicillin/streptomycin) containing different test compounds for 24 h. Neuro-2a cells were captured and counted under a phase contrast microscope. Neurites were defined as a protrusion with lengths longer than one diameter of the cell body. The neurite length of each cell was measured by Image J software.

### 3.6 Protein extraction and western blot analysis

Neuro-2a cells were seeded in 35 mm dish ( $6 \times 10^4$ /dish) overnight and then incubated with compound A5 for different time (0–240 min) at 37 °C. Cells were lysed in RIPA buffer containing protease and phosphatase inhibitors and whole cell lysates were quantified using a BCA protein assay kit according to the manufacturer's instructions. Those cell lysates were subsequently separated by SDS-PAGE, and transferred to PVDF membranes. The membranes were probed with primary antibody, and then subsequently with secondary antibody, followed by electrochemiluminescence (ECL) detection. The following primary antibodies were used: P-Akt (Ser473) (#AA329), Akt (#AA326), P-ERK1/2 (#AF1891), ERK1/2 (#AF1051), P-p38



(#AM063), p38 (#AF1111), P-JNK1/2/3 (#AF1762), JNK1/2/3 (#AF1048) and  $\beta$ -actin (#AA128) antibodies. The antibodies and secondary antibody (#A0216, #A0208) were all purchased from Beyotime (Jiangsu, China)

### 3.7 Statistical analysis

The results are expressed as the mean  $\pm$  standard error of the mean (SEM). Data were subjected to Student's *t* test or oneway analysis of variance (ANOVA) followed by Tukey's test to assess the differences between the relevant control and each experimental group. A value of  $P < 0.05$  was considered statistically significant.

## 4. Conclusions

In this work, several acylhydrazone derivatives (**A0–A10**) have been designed and synthesized, among them two newly synthesized compounds (**A6**, **A8**). All of the compounds were evaluated for neuritogenic activity in Neuro-2a cells. The pharmacological results indicated that compound **A5** exhibit highly potent neuritogenic activity through the PI3K/Akt and MEK-ERK signaling pathway *in vitro*. The above results suggested that compound **A5** hold high potential use for treating neural injury and neurodegenerative diseases.

## Conflicts of interest

The authors declare that they have no conflict interests.

## Acknowledgements

This work was financially supported by the Research Foundation of Education Department of Hunan Province, China (No. 17A66, No. 17B208), and the National Natural Science Foundation of China (No. 31900705, No. 81703821), as well as the Foundation of Hunan Double First-rate Discipline Construction Projects of Bioengineering (No. YYZW2019-04).

## References

- 1 H. Takahashi, K. Matsuda, K. Tabuchi and J. Ko, Central synapse, neural circuit, and brain function, *Neurosci. Res.*, 2017, **116**, 1–2.
- 2 F. M. Gafarov, Neural electrical activity and neural network growth, *Neural Network.*, 2018, **101**, 15–24.
- 3 T. T. Chuang, Neurogenesis in mouse models of Alzheimer's disease, *Biochim. Biophys. Acta*, 2010, **1802**, 872–880.
- 4 M. W. Marlatt and P. J. Lucassen, Neurogenesis and Alzheimer's disease: Biology and pathophysiology in mice and men, *Curr. Alzheimer Res.*, 2010, **7**, 113–125.
- 5 J. A. Korecka, S. Talbot, T. M. Osborn, S. M. de Leeuw, S. A. Levy, E. J. Ferrari, A. Moskites, E. Atkinson, F. M. Jodelka, A. J. Hinrich, M. L. Hastings, C. J. Woolf, P. J. Hallett and O. Isacson, Neurite Collapse and Altered ER Ca(2+) Control in Human Parkinson Disease Patient iPSC-Derived Neurons with LRRK2 G2019S Mutation, *Stem Cell Rep.*, 2019, **12**, 29–41.
- 6 N. Kurup, P. Sharifnia and Y. Jin, Spatial and temporal dynamics of neurite regrowth, *Curr. Opin. Neurobiol.*, 2013, **23**, 1011–1017.
- 7 S. V. More, S. Koppula, I. S. Kim, H. Kumar, B. W. Kim and D. K. Choi, The role of bioactive compounds on the promotion of neurite outgrowth, *Molecules*, 2012, **17**, 6728–6753.
- 8 G. Tang, X. Liu, N. Ma, X. Huang, Z. L. Wu, W. Zhang, Y. Wang, B. X. Zhao, Z. Y. Wang, F. C. Ip, N. Y. Ip, W. C. Ye, L. Shi and W. M. Chen, Design and Synthesis of Dimeric Securinine Analogues with Neuritogenic Activities, *ACS Chem. Neurosci.*, 2016, **7**, 1442–1451.
- 9 L. Pol-Fachin, C. A. Fraga, E. J. Barreiro and H. Verli, Characterization of the conformational ensemble from bioactive N-acylhydrazone derivatives, *J. Mol. Graphics Modell.*, 2010, **28**, 446–454.
- 10 C. Maia Rdo, R. Tesch and C. A. Fraga, Acylhydrazone derivatives: a patent review, *Expert Opin. Ther. Pat.*, 2014, **24**, 1161–1170.
- 11 P. Melnyk, V. Leroux, C. Sergheraert and P. Grellier, Design, synthesis and *in vitro* antimalarial activity of an acylhydrazone library, *Bioorg. Med. Chem. Lett.*, 2006, **16**, 31–35.
- 12 A. C. Lannes, B. Leal, J. S. Novais, V. Lione, G. C. Monteiro, A. L. Lourenco, P. C. Sathler, A. K. Jordao, C. R. Rodrigues, L. M. Cabral, A. C. Cunha, V. Campos, V. F. Ferreira, M. C. de Souza, D. O. Santos and H. C. Castro, Exploring N-acylhydrazone derivatives against clinical resistant bacterial strains, *Curr. Microbiol.*, 2014, **69**, 357–364.
- 13 L. N. Cardoso, M. L. Bispo, C. R. Kaiser, J. L. Wardell, S. M. Wardell, M. C. Lourenco, F. A. Bezerra, R. P. Soares, M. N. Rocha and M. V. de Souza, Anti-tuberculosis evaluation and conformational study of N-acylhydrazones containing the thiophene nucleus, *Arch. Pharm.*, 2014, **347**, 432–448.
- 14 Y. K. da Silva, C. V. Augusto, M. L. de Castro Barbosa, G. M. de Albuquerque Melo, A. C. de Queiroz, T. de Lima Matos Freire Dias, W. B. Junior, E. J. Barreiro, L. M. Lima and M. S. Alexandre-Moreira, Synthesis and pharmacological evaluation of pyrazine N-acylhydrazone derivatives designed as novel analgesic and anti-inflammatory drug candidates, *Bioorg. Med. Chem.*, 2010, **18**, 5007–5015.
- 15 J. C. Silva, R. G. Oliveira Junior, M. G. E. Silva, E. M. Lavor, J. M. D. Soares, S. R. G. Lima-Saraiva, T. C. Diniz, R. L. Mendes, E. B. Alencar Filho, E. J. L. Barreiro, L. M. Lima and J. Almeida, LASSBio-1586, an N-acylhydrazone derivative, attenuates nociceptive behavior and the inflammatory response in mice, *PLoS One*, 2018, **13**, e0199009.
- 16 J. V. Cerqueira, C. S. Meira, E. S. Santos, L. S. de Aragao Franca, J. F. Vasconcelos, C. K. V. Nonaka, T. L. de Melo, J. M. Dos Santos Filho, D. R. M. Moreira and M. B. P. Soares, Anti-inflammatory activity of SintMed65, an N-acylhydrazone derivative, in a mouse model of allergic airway inflammation, *Int. Immunopharmacol.*, 2019, **75**, 105735.





- 17 B. Tian, M. He, Z. Tan, S. Tang, I. Hewlett, S. Chen, Y. Jin and M. Yang, Synthesis and antiviral evaluation of new N-acylhydrazones containing glycine residue, *Chem. Biol. Drug Des.*, 2011, **77**, 189–198.
- 18 B. Tian, M. He, S. Tang, I. Hewlett, Z. Tan, J. Li, Y. Jin and M. Yang, Synthesis and antiviral activities of novel acylhydrazone derivatives targeting HIV-1 capsid protein, *Bioorg. Med. Chem. Lett.*, 2009, **19**, 2162–2167.
- 19 X. Yu, L. Shi and S. Ke, Acylhydrazone derivatives as potential anticancer agents: Synthesis, bio-evaluation and mechanism of action, *Bioorg. Med. Chem. Lett.*, 2015, **25**, 5772–5776.
- 20 Y. F. He, M. L. Nan, Y. W. Zhao, W. Y. Sun, W. Li and Q. C. Zhao, Design, synthesis and evaluation of antitumor activity of new rotundic acid acylhydrazone derivatives, *Z. Naturforsch., C: J. Biosci.*, 2016, **71**, 95–103.
- 21 S. Rupiani, R. Buonfiglio, M. Manerba, L. Di Ianni, M. Vettriano, E. Giacomini, M. Masetti, F. Falchi, G. Di Stefano, M. Roberti and M. Recanatini, Identification of N-acylhydrazone derivatives as novel lactate dehydrogenase A inhibitors, *Eur. J. Med. Chem.*, 2015, **101**, 63–70.
- 22 F. Miller, U. Hinze, B. Chichkov, W. Leibold, T. Lenarz and G. Paasche, Validation of eGFP fluorescence intensity for testing in vitro cytotoxicity according to ISO 10993-5, *J. Biomed. Mater. Res., Part B*, 2017, **105**, 715–722.
- 23 Y. An, T. Zhang, H. Jiang, L. Zhang, J. Han and M. X. Yao, Synthesis, Structure and Their Biological Activities of 3-[(5-H/methyl-benzimidazol-2-yl) methylthio]-5-substituted-1,2,4-triazol-4-amine Derivatives, *Chin. J. Org. Chem.*, 2012, **32**, 1308–1313.
- 24 J. Han, X. X. Zhou, S. B. Chen and Y. An, Synthesis and Biological Activities of Novel Acylhydrazone Containing 1,2,4-Triazole Structure, *Chin. J. Org. Chem.*, 2014, **34**, 741–748.

